Journal of Coordination Chemistry

ISSN: 0095-8972 (Print) 1029-0389 (Online) Journal homepage: http://www.tandfonline.com/loi/gcoo20

Synthesis, structures, and electroluminescence properties of a 1D zinc(II) coordination polymer containing both dicyanamide and pyrazinamide ligands

Leila Tabrizi, Hossein Chiniforoshan & Patrick Mcardle

To cite this article: Leila Tabrizi, Hossein Chiniforoshan & Patrick Mcardle (2015) Synthesis, structures, and electroluminescence properties of a 1D zinc(II) coordination polymer containing both dicyanamide and pyrazinamide ligands, Journal of Coordination Chemistry, 68:11, 1936-1946, DOI: 10.1080/00958972.2015.1036749

To link to this article: http://dx.doi.org/10.1080/00958972.2015.1036749

Accepted author version posted online: 07 Apr 2015.
Published online: 28 Apr 2015.

Journal of Coordination Chemistry, 2015
Vol. 68, No. 11, 1936–1946, http://dx.doi.org/10.1080/00958972.2015.1036749

Synthesis, structures, and electroluminescence properties of a 1D zinc(II) coordination polymer containing both dicyanamide and pyrazinamide ligands

LEILA TABRIZI†, HOSSEIN CHINIFOROSHAN*† and PATRICK MCARDLE‡

†Department of Chemistry, Isfahan University of Technology, Isfahan, Iran
‡School of Chemistry, National University of Ireland Galway, Galway, Ireland

(*Received 27 September 2014; accepted 23 February 2015*)

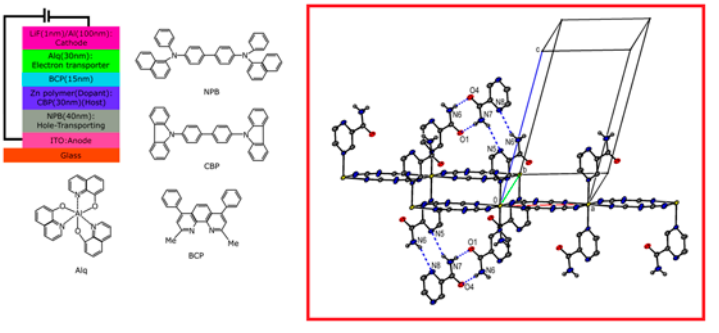

A 1D coordination polymer, $\{[Zn(\mu_{1,5}\text{-dca})_2(PZA)_2](PZA)_2\}_n$ (**1**), has been synthesized and characterized by single-crystal X-ray crystallography. The coordination modes of the dicyanamide (dca) and the pyrazinamide (PZA) were inferred by IR spectroscopy. The complex was applied to organic electroluminescent (EL) devices as the emitting materials. The electroluminescent device of ITO/NPB (40 nm)/Zn polymer: CBP (30 nm) (30 nm)/BCP (15 nm)/Alq (30 nm)/LiF (1 nm)/Al (100 nm) was fabricated. The EL device emits cyan light originating from this complex with high brightness and efficiencies. For **1**, a maximum luminance of 34.9 cd/A was achieved at 9 V.

Keywords: Zinc(II); Dicyanamide; Pyrazinamide; Electroluminescence

1. Introduction

The design of coordination polymers (CPs) has attracted attention in supramolecular chemistry and crystal engineering for intriguing architectural topologies [1–4] and applications as functional materials and in luminescence [5–8].

*Corresponding author. Email: Chinif@cc.iut.ac.ir

Luminescent organic/organometallic compounds have attracted attention owing to potential applications in flat panel displays based on organic light-emitting diodes (OLEDs). These materials are useful in OLEDs because of relatively high stability and efficiency [9, 10].

The d^{10} metal ions possess various coordination numbers and geometries and attractive luminescent properties when bound to functional ligands, representing desirable synthetic targets [11–14]. Zinc complexes have been especially important because of the simplicity in synthesis and wide spectral investigations. Considerable research is carried on in various laboratories to synthesize zinc complexes containing new ligands to produce a number of luminescent zinc complexes [15–20] as emitters and electron transporters in OLED research [21–23]. However, low thermal stability of this type of material limits applications, especially in the area of LEDs [24]. To overcome the problem, we chose CPs to construct OLEDs. As hybrid materials, CPs have relatively rigid skeletons which offer excellent thermal stability [25–28]. Coordination with metal ions often enhances the rigidity of the linker, increasing fluorescence intensity [29–31].

Dicyanamide (dca) is a versatile [32–35] bridging unit and may bind metal ions as terminal or bridging ligands; dca is non-fluorescent, but its assembly generates highly interesting fluorescent CPs [36].

There is an analogy between the emission behavior of pyrazinamide (PZA) and 8-hydroxyquinoline since both ligands have similar chromophoric groups, i.e. a coordinating imine and a delocalized π system [37]. Therefore, zinc(II) complexes of pyrazinamide are expected to show good luminescence, enhancing the quantum yield of photoluminescence.

In this report, we synthesized a 1D compound of zinc(II) with dca and PZA, $\{[Zn(\mu_{1,5}\text{-dca})_2(PZA)_2](PZA)_2\}_n$ (**1**), and its optical and photoluminescence (PL) properties have been investigated. An organic light-emitting device was fabricated using the complex as emitting layer to study its electroluminescence (EL) properties. The device based on the complex gave high brightness and external quantum efficiencies. Also, details of syntheses, spectroscopic characterizations and X-ray structure of this complex are described below.

2. Experimental

2.1. *Materials*

All chemicals and solvents were purchased from Merck or Sigma-Aldrich and used without any further purification. Pyrazinamide was obtained from the Abidi Pharmaceutical Company.

2.2. *Physical measurements*

Fourier transform infrared spectra were recorded on a FT-IR JASCO 680-PLUS spectrometer from 4000 to 400 cm^{-1} using KBr pellets. Elemental analyses were performed using a Leco, CHNS-932 elemental analyzer. The UV–vis spectra were recorded on a UV-JASCO-570 spectrometer. PL spectra were recorded on a Perkin–Elmer LS 50B luminescence spectrophotometer. Current, voltage, and light-intensity measurements were made simultaneously using a Keithley 2400 source meter and a Newport 1835-C optical meter equipped with a Newport 818-ST silicon photodiode.

2.3. *Synthesis of {[Zn(μ$_{1,5}$-dca)$_2$(PZA)$_2$](PZA)$_2$}$_n$ (1)*

An aqueous solution (10 cm^3) of $Zn(OAc)_2{\cdot}2H_2O$ (216 mg, 1.0 mmol) and $NaN(CN)_2$ (178.06 mg, 2.0 mmol) was stirred for 10 min, and an aqueous solution (50 cm^3) of PZA (492.4 mg, 4.0 mmol) was added dropwise. After filtration, the filtrate was then left to evaporate slowly. Colorless single crystals were obtained after several weeks. Yield: 72%. Elemental analyses were in agreement with the $C_{12}H_{10}Zn_{0.5}N_9O_2$ stoichiometry for **1**. Found (Calcd %): C, 41.71 (41.78); N, 36.49 (36.54); H, 2.84 (2.92). IR data on KBr (ν, cm^{-1}) pellets: ν (NH_2): 3414 (s); ν (aromatic C–H): 3069 (w); $\nu_s + \nu_{as}$(C≡N): 2325 (s); ν_{as} (C≡N): 2246 (s); ν_s (C≡N): 2179 (s); ν (C=O): 1709 (vs); ν (C=N): 1576 (s), ν (C=C): 1419 (s); ν_a (C–N)(dca): 1383; ν (ring breathing): 1090.

2.4. *OLED fabrication*

The OLED device was fabricated in a configuration ITO/NPB (40 nm)/Zn polymer: CBP (30 nm)/BCP (15 nm)/Alq (30 nm)/LiF (1 nm)/Al (100 nm). Indium tin oxide (ITO)-coated glass substrates with sheet resistance of 25 Ω^{-2} were patterned and cleaned using trichloroethylene, acetone, isopropyl alcohol, and deionized water sequentially for 20 min using an ultrasonic bath and dried in flowing nitrogen. On the substrate, the hole transport layer and the emitting layers were deposited sequentially under a high vacuum (1×10^{-5} Torr) at a deposition rate of 1 Å/s and LiF at 0.5 Å/s. Thickness of the deposited layers were controlled by a quartz crystal monitor.

2.5. *Crystal structure determination*

Relevant results from data collection and structure solution are summarized in table 1. Crystals of **1** were grown by slow evaporation from methanol solution. An Oxford Diffraction Xcalibur system was used to collect X-ray diffraction data. The crystal structures were

Table 1. Crystallographic data for **1**.

Empirical formula	$C_{12}H_{10}N_9O_2Zn_{0.50}$
Formula weight	344.97
T/K	293 (2) K
Crystal system	Triclinic
Space group	Pī
a/Å	7.4303(9)
b/Å	7.5983(9)
c/Å	14.527(2)
α/°	75.577(13)
β/°	78.660(12)
γ/°	62.916(12)
V/Å^3	703.93(19)
Z	2
μ (mm^{-1})	0.94
D_{cal}/Mg m^{-3}	1.628
F(0 0 0)	352
θ Range/°	3.1–29.1
Independent reflections	2924 [R(int) = 0.1002]
Data/restraints/parameters	2924/159/214
Goodness-of-fit on F^2	0.990
Final R indices	R_1 = 0.0758, wR_2 = 0.1672
R indices (all data)	R_1 = 0.1462, wR_2 = 0.1945
Largest diff. peak and hole (e Å^{-3})	1.030, −0.844

solved by direct methods (Shelxt2014) and refined by full matrix least squares using Shelxl2014 within the Oscail package [38, 39]. Non-hydrogen atoms were refined anisotropically.

3. Results and discussion

3.1. *Synthesis and spectroscopic study of 1*

The synthesis of **1** in high yield was achieved via aerobic reaction of dca and PZA with Zn $(OAc)_2 \cdot 2H_2O$ in aqueous solution. Complex **1** is soluble in DMSO and DMF.

PZA can coordinate through the pyrazine ring nitrogens and the C=O or $-NH_2$ groups. IR spectroscopy can be indicative of the coordination mode of PZA in complexes. The coordination mode of PZA in **1** was examined by comparing spectra of free and complexed PZA. The strong absorption at 3414 cm^{-1}, observed in the spectra of free PZA and in the spectra of **1**, is assigned to the ν (NH_2) mode of the amino terminal group [40]. The lack of shift in ν (NH_2) suggests that PZA does not coordinate to the metal in these complexes through nitrogen of NH_2. The strong band at 1709 cm^{-1} observed in spectra of **1** was attributed to the ν(CO) mode of coordinated PZA, which appears at 1712 (IR) cm^{-1} in free PZA. Therefore, it also does not take part in coordination. In the IR spectra, the ring-breathing

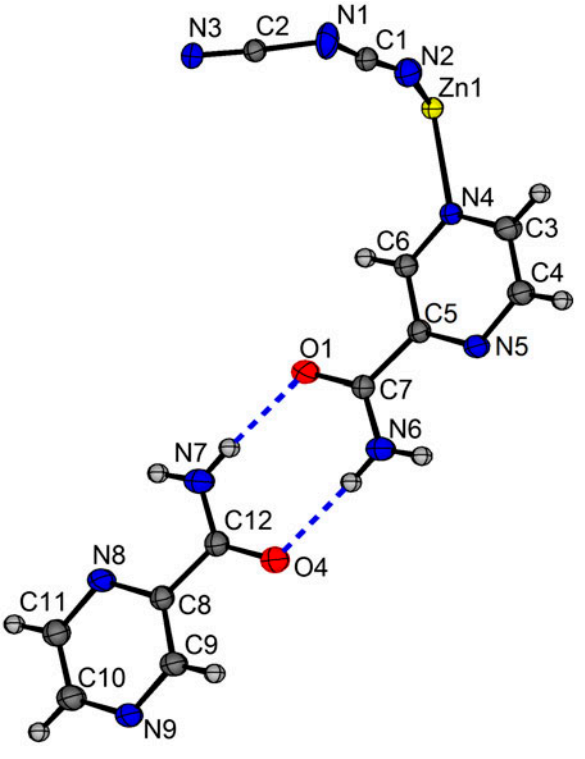

Figure 1. ORTEX drawing with the atom-labeling of the asymmetric unit, 40% ellipsoids, for **1**.

mode of PZA is at 1025 cm^{-1} for solid PZA and 1045 cm^{-1} for **1**. The blue shift of ring breathing suggests the PZA is coordinated in **1** through the heterocyclic ring nitrogen [41–44].

The IR spectrum of **1**, as shown in the Experimental section, has a profile that is determined to a large extent by dca. There are strong absorptions at 2325, 2246, and 2179 cm^{-1}, corresponding to the $\nu_s + \nu_{as}$ (C≡N), ν_{as} (C≡N), and ν_s (C≡N) modes of the dca ligand, respectively [45]. The shift toward higher frequencies of these peaks, when compared with those of the free dca in its sodium salt (strong peaks at 2286, 2232, and 2129 cm^{-1}), is

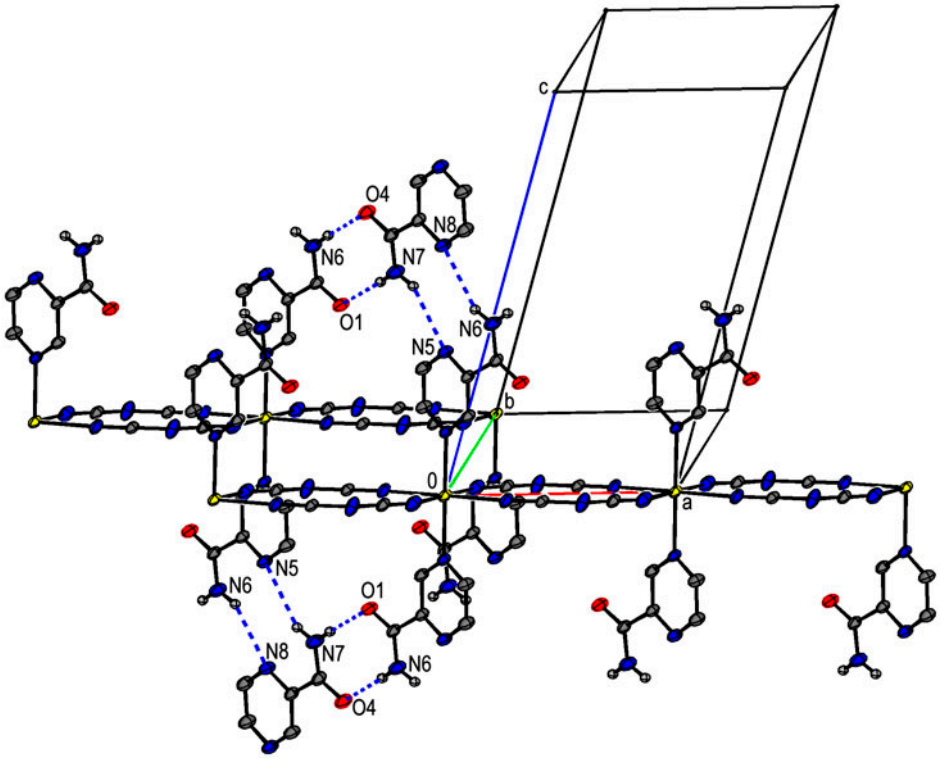

Figure 2. Packing diagram of **1**; hydrogen bonds are represented by dotted lines; hydrogens not involved in hydrogen bonding are omitted for clarity.

Table 2. Hydrogen bonds for **1** [Å and °].

D-H···A	d(D–H)	d(H···A)	d(D···A)	<(DHA)
N(6)–H(6A)···O(4)	0.86	2.07	2.926(7)	177.1
N(6)–H(6B)···N(8)#5	0.86	2.42	3.118(8)	138.4
N(7)–H(7A)···O(1)	0.86	2.03	2.890(7)	175.8
N(7)–H(7B)···N(5)#6	0.86	2.48	3.180(8)	139.3

Symmetry transformations used to generate equivalent atoms: #1 $-x-1, -y, -z$; #2 $x+1, y, z$; #3 $-x, -y, -z$; #4 $x-1, y, z$; #5 $x+1, y-1, z$; #6 $x-1, y+1, z$.

consistent with the coordination of the ligand. Bands from ν_{as} (C–N) (1400–1300 cm^{-1}) and ν_s (C–N) (950–900 cm^{-1}) also occur in spectra of **1**.

3.2. *Structural description of 1*

The crystal was twinned; however, a twin component extraction procedure was successfully used to obtain and interpret the data. The asymmetric unit of **1** is shown in figure 1; the complex is composed of linear chains of zinc ions bridged by end-to-end dca ligands and coordinated by PZA ligands, figure 2. Each zinc is connected to two neighbors by four equatorially bound dca ligands, which participate in two successive $Zn(dca)_2Zn$ units. Two nitrile nitrogens in dca are involved in coordination, so dca is a bridge in a μ-1,5 mode. The slightly distorted octahedral coordination spheres of Zn ions are completed by the coordination of two monodentate *trans* PZA ligands. The $Zn\text{-}N_{dicyan}$ equatorial distances [2.097(5) and 2.112(5) Å], average 2.1045 Å, are shorter than the $Zn\text{-}N_{PZA}$ axial lengths of 2.233(5) Å. The ZnN_6 octahedron is only slightly distorted as shown by the near 90° values for the *cis*-N-Zn-N′ angles, which are 87.4(2) and 92.6(2)°. Polymeric 1-D chains are generated parallel to the *a*-axis, with adjacent chains staggered *a*/2 so as to provide a more

Table 3. Selected bond distances (Å) and angles (°) for **1**.

Zn(1)–N(3)	2.097(5)	Zn(1)–N(2)	2.112(5)
Zn(1)–N(4)	2.333(5)	O(1)–C(7)	1.232(7)
O(4)–C(12)	1.237(7)	N(6)–C(7)	1.302(8)
N(7)–C(12)	1.308(83)	N(4)–C(3)	1.328(7)
N(3)–Zn(1)–N(3)	180.0(6)	N(3)–Zn(1)–N(2)	87.4(2)
N(2)–Zn(1)–N(2)	180.0	N(3)–Zn(1)–N(4)	90.08(18)
N(2)–Zn(1)–N(4)	90.6(2)	N(4)–Zn(1)–N(4)	180.0
C(3)–N(4)–Zn(1)	122.1(4)	C(6)–N(4)–Zn(1)	121.5(4)
C(2)–N(3)–Zn(1)	162.5(5)	C(1)–N(2)–Zn(1)	152.0(5)
N(1)–C(1)–N(2)	172.4(6)	N(3)–C(2)–N(1)	173.2(7)
C(2)–N(1)–C(1)	123.6(6)		

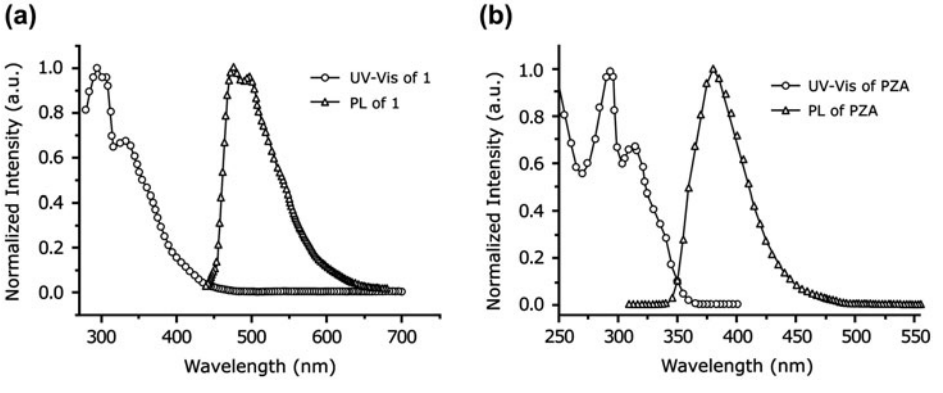

Figure 3. The UV–vis absorption and photoluminescence spectra of (a) **1** in DMF and (b) PZA in methanol.

efficient packing arrangement (see figure 2). Weak π–π interactions are evident, with the distance between pyrazine ring centroids being 3.673 Å and a β offset angle of 108.37°.

In the crystal structure, there are N–H···O and N–H···N hydrogen bonds which are listed in table 2 and illustrated in figure 2. The oxygen is a bifurcated acceptor, simultaneously accepting an amide hydrogen of PZA [N–H–O, 2.926(7) Å; symmetry code: $-x + 1, -y, -z$]. The selected bond distances and angles of **1** are collected in table 3.

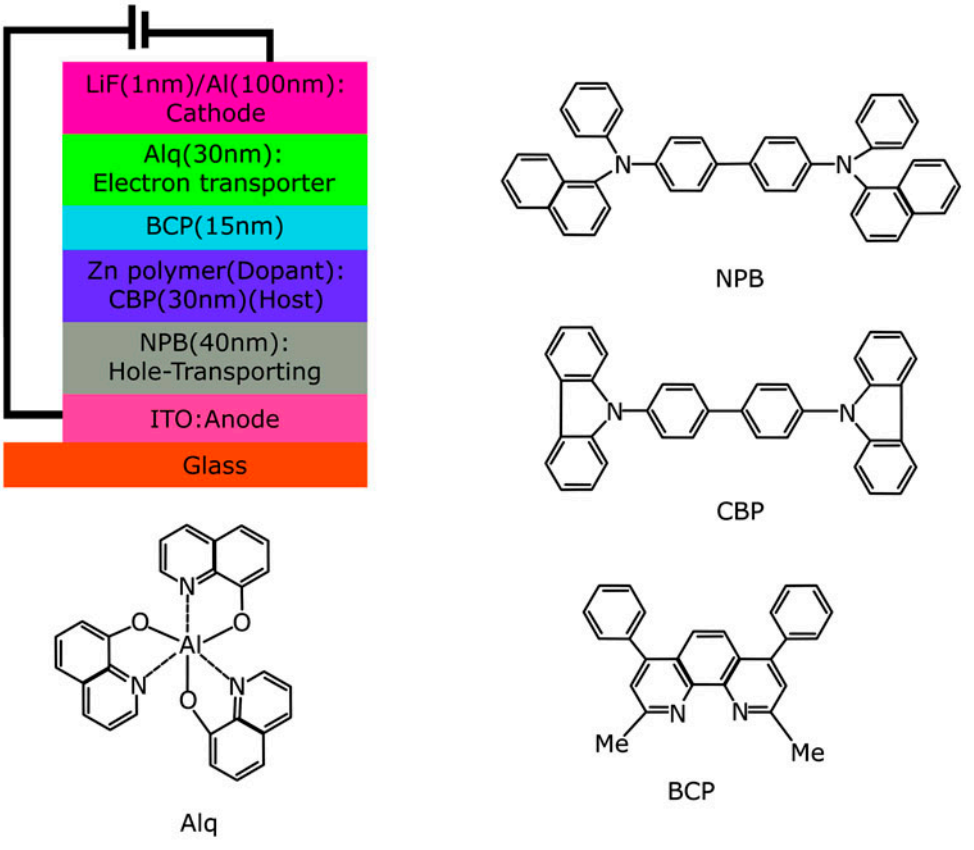

Figure 4. The general structure of the device and the molecular structures of the compounds used in the device.

Table 4. Performance data of the Zn polymer-based OLEDs.

Device	Turn-on voltage (V)	η_{ext} (%, V)	L (cd/m^2, V)	η_c (cd/A, V)	η_p (I_m/W, V)	λ_{max} (nm)	CIE, 8 V (x, y)
A: 6.6% Zn polymer	3.1	12.1, 9.0	41,100, 17.7	34.9, 9.0	14.7, 4.8	491	(0.21, 0.53)

Note: The data for external quantum efficiency (η_{ext}), brightness (L), current efficiency (η_c), and power efficiency (η_p) are the maximum values of the device.

3.3. *Absorption and emission*

Figure 3(a) and (b) illustrates the UV–vis and photoluminescence (PL) spectra of **1** in DMF and PZA in methanol at room temperature. In figure 3(a), there are two major absorptions at 297 and 342 nm in the UV–vis spectrum. Since the zinc ion has d^{10} configuration, the bands could be assigned to intraligand transitions. On irradiation with 340 nm, light **1** showed photoluminescence in DMF at 473 nm, falling in blue to cyan region. In figure 3(b), the strong absorption band at 250–350 nm can be assigned to π–π^* transition in PZA. The PL emission peak of PZA in methanol was observed at 380 nm. Although dicyanamide and the metal salt are non-fluorescent [36], the assembly causes highly interesting fluorescent CPs. We consider that the emission of **1** is PZA-based, involving the most likely $^1(\pi$–$\pi^*)$ transitions.

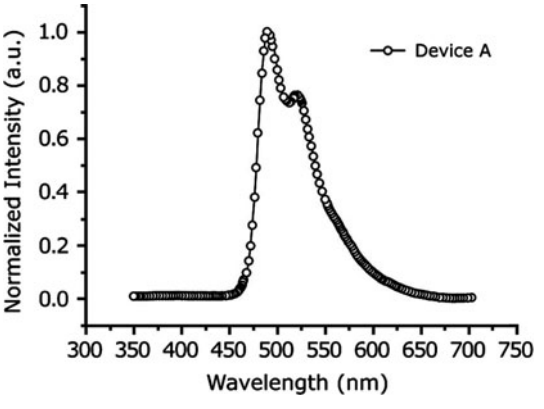

Figure 5. The electroluminescence spectra of the device.

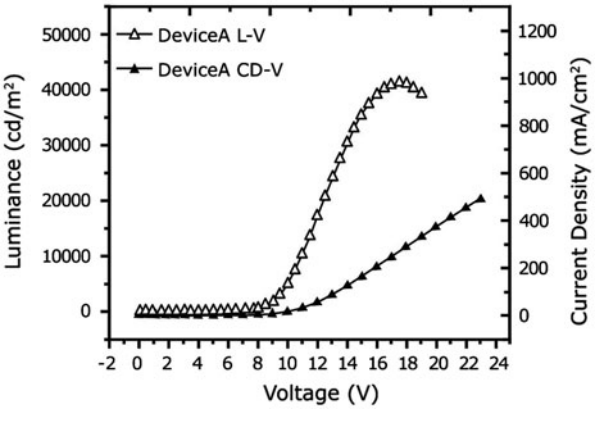

Figure 6. The luminance–voltage–current (*L*–*V*–*I*) characteristics of the device.

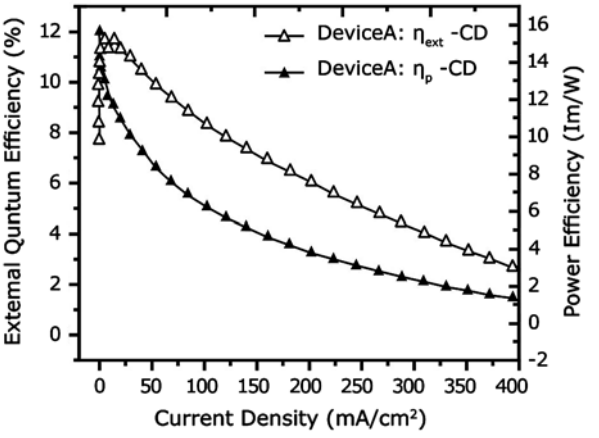

Figure 7. The external quantum efficiency (η_{ext})–current density–power efficiency (η_p) characteristics of the device.

3.4. *Electroluminescent properties*

To illustrate the electroluminescent properties of **1**, typical OLED device (device A) using **1** as dopant was fabricated. The device had a multi-layer configuration ITO/NPB (40 nm)/Zn polymer: CBP (30 nm)/BCP (15 nm)/Alq (30 nm)/LiF (1 nm)/Al (100 nm), in which ITO (indium tin oxide) was used as the anode, NPB (4,4′-bis[N-(1-naphthyl)-N-phenylamino] biphenyl) was used as the hole-transporting material, CBP (4,4′-N,N′-dicarbozole biphenyl) as the host, the Zn polymer as dopant, Alq (tris(8-hydroxyquinolinato) aluminum) as the electron transporter, and LiF/Al as the cathode (figure 4). Key characteristics of this device are listed in table 4.

Device A emitted strong cyan light with an emission maximum at 491 nm (figure 5). The EL spectrum of the device does not change significantly with variation of the applied voltages from 6 to 12 V. Based on the EL spectrum at an applied voltage of 8 V, the Commission International de I'Eclairage (CIE) coordinates of device A are (0.21, 0.53). The CIE coordinate of this complex is almost independent of driving voltage.

Figures 6 and 7 show the luminance–voltage–current (*L–V–I*) and the external quantum efficiency (η_{ext})–current density–power efficiency (η_p) characteristics of the device, respectively. Device A showed quite high efficiencies and brightness. For the device, with 6.6% of **1** as dopant, an extremely high external quantum efficiency of 12.1%, a maximum brightness of 41,100 cd/m^2 at 17.7 V, and a current efficiency of 34.9 cd/A were achieved (table 4).

4. Conclusion

A 1D Zn(II) polymer, $\{[Zn(\mu_{1,5}\text{-dca})_2(PZA)_2](PZA)_2\}_n$ (**1**), containing dicyanamide (dca) and the pyrazinamide (PZA) ligands was synthesized and characterized by single crystal X-ray crystallography and IR spectroscopy. PZA coordinated to Zn(II) through the

heterocyclic ring nitrogen. The EL device based on this complex emitted cyan color, with high brightness and efficiencies for organic light-emitting device application.

Acknowledgments

We are grateful for the financial support from the Department of Chemistry, Isfahan University of Technology (IUT). Also, the authors would like to thank Abidi Pharmacological Company for providing us with the required Pyrazinamide.

Disclosure statement

No potential conflict of interest was reported by the authors.

References

[1] A.M. Kirillov. *Coord. Chem. Rev.*, **255**, 1603 (2011).
[2] S. Wang, X.-H. Ding, J.-L. Zuo, X.-Z. You, W. Huang. *Coord. Chem. Rev.*, **255**, 1713 (2011).
[3] C.J. Sumby. *Coord. Chem. Rev.*, **255**, 1937 (2011).
[4] Z.M. Hao, X.M. Zhang. *Cryst. Growth Des.*, **7**, 64 (2007).
[5] J.-R. Li, Y. Ma, M.C. McCarthy, J. Sculley, J. Yu, H.-K. Jeong, P.B. Balbuena, H.-C. Zhou. *Coord. Chem. Rev.*, **255**, 1791 (2011).
[6] Z. Ma, B. Moulton. *Coord. Chem. Rev.*, **255**, 1623 (2011).
[7] D.K. Dutta, B. Deb. *Coord. Chem. Rev.*, **255**, 1686 (2011).
[8] S.-L. Zheng, J.-P. Zhang, W.-T. Wong, X.-M. Chen. *J. Am. Chem. Soc.*, **125**, 6882 (2003).
[9] C.W. Tang, S.A. VanSlyke. *Appl. Phys. Lett.*, **51**, 913 (1987).
[10] C.W. Tang, S.A. VanSlyke, C.H. Chen. *J. Appl. Phys.*, **65**, 3610 (1989).
[11] Q. Chu, G.X. Liu, Y.-Q. Huang, X.-F. Wang, W.Y. Sun. *Dalton Trans.*, **38**, 4302 (2007).
[12] Q. Fang, G. Zhu, M. Xue, J. Sun, F. Sun, S. Qiu. *Inorg. Chem.*, **45**, 3582 (2006).
[13] C.A. Bauer, T.V. Timofeeva, T.B. Settersten, B.D. Patterson, V.H. Liu, B.A. Simmons, M.D. Allendorf. *J. Am. Chem. Soc.*, **129**, 7136 (2007).
[14] M.-S. Wang, S.-P. Guo, Y. Li, L.-Z. Cai, J.-P. Zou, G. Xu, W.-W. Zhou, F.-K. Zheng, G.-C. Guo. *J. Am. Chem. Soc.*, **131**, 13572 (2009).
[15] Y. Hamada, T. Sano, M. Fujita, T. Fujii, Y. Nishio, K. Shibata. *Jpn. J. Appl. Phys.*, **32**, L514 (1993).
[16] J. Kido, K. Hongawa, K. Okuyama, K. Nagai. *Appl. Phys. Lett.*, **64**, 815 (1994).
[17] Y. Hamada, T. Sano, H. Fujii, Y. Nishio, H. Takahashi, K. Shibata. *Jpn J. Appl. Phys.*, **35**, L1339 (1996).
[18] S.F. Liu, Q. Wu, H.L. Schmider, H. Aziz, N.X. Hu, S. Wang, Z. Popovic. *J. Am. Chem. Soc.*, **122**, 3671 (2000).
[19] Q. Wu, J.A. Lavigne, S. Wang. *Inorg. Chem.*, **39**, 5248 (2000).
[20] Y.K. Jang, D.E. Kim, O.K. Kwon, Y.S. Kwon. *J. Korean Phys. Soc.*, **49**, 1057 (2006).
[21] N. Donze, P. Pechy, M. Gratzel, M. Schaer, L. Zuppiroli. *Chem. Phys. Lett.*, **315**, 405 (1999).
[22] A.N. Du, Q. Mei, M. Lu. *Synth. Met.*, **149**, 193 (2005).
[23] A. Yeh, T.R. Chen. *Mater. Lett.*, **59**, 2911 (2005).
[24] M. Meneghini, L.-R. Trevisanello, F. de Zuani, N. Trivellin, G. Meneghesso, E. Zanoni. *SPIE Ninth International Conference on Solid State Lighting*, **7422**, 74220H (2009).
[25] D. Banerjee, L.A. Borkowski, S.J. Kim, J.B. Parise. *Cryst. Growth Des.*, **9**, 4922 (2009).
[26] C. Pan, J.-P. Nan, X.-L. Dong, X.-M. Ren, W.-Q. Jin. *J. Am. Chem. Soc.*, **133**, 12330 (2011).
[27] M. Gustafsson, A. Bartoszewicz, B. Martín-Matute, J.-L. Sun, J. Grins, T. Zhao, Z.-Y. Li, G.-S. Zhu, X.-D. Zou. *Chem. Mater.*, **22**, 3316 (2010).
[28] C.-Y. Sun, S.-X. Liu, D.-D. Liang, K.-Z. Shao, Y.-H. Ren, Z.-M. Su. *J. Am. Chem. Soc.*, **131**, 1883 (2009).
[29] M.D. Allendorf, C.A. Bauer, R.K. Bhaktaa, R.J.T. Houka. *Chem. Soc. Rev.*, **38**, 1330 (2009).
[30] V.J. Catalano, A.L. Moore. *Inorg. Chem.*, **44**, 6558 (2005).
[31] S.-L. Zheng, J.-H. Yang, X.-L. Yu, X.-M. Chen, W.-T. Wong. *Inorg. Chem.*, **43**, 830 (2004).
[32] S.R. Batten, K.S. Murray. *Coord. Chem. Rev.*, **246**, 103 (2003).
[33] Y.-F. Yue, E.-Q. Gao, C.-J. Fang, S. Xu, C.-H. Yan. *J. Mol. Struct.*, **841**, 67 (2007).

[34] F.A. Mautner, M. Mikuriya, H. Ishida, H. Sakiyama, F.R. Louka, J.W. Humphrey, S.S. Massoud. *Inorg. Chim. Acta*, **362**, 4073 (2009).
[35] S.S. Massoud, F.R. Louka, M. Mikuriya, H. Ishida, F.A. Mautner. *Inorg. Chem. Commun.*, **12**, 420 (2009).
[36] P. Chakraborty, S. Mondal, S. Das, A.D. Jana, D. Das. *Polyhedron*, **70**, 11 (2014).
[37] T. Yu, W. Su, W. Li, Z. Hong, R. Hua, M. Li, B. Chu, B. Li, Z. Zhang, Z.Z. Hu. *Inorg. Chim. Acta*, **359**, 2246 (2006).
[38] G. Sheldrick. *Acta Crystallogr., Sect. A*, **64**, 112 (2008).
[39] P. McArdle, K. Gilligan, D. Cunningham, R. Dark, M. Mahon. *Cryst. Eng. Comm.*, **6**, 303 (2004).
[40] E. Akalin, S. Akyuz. *J. Mol. Struct.*, **834–836**, 492 (2007).
[41] S. Akyuz, A.B. Dempster, R.L. Morehouse, S. Suzuki. *J. Mol. Struct.*, **17**, 105 (1973).
[42] T. Akyuz, S. Akyuz, J.E.D. Davies. *J. Inclusion Phenom. Mol. Recognit. Chem.*, **9**, 349 (1990).
[43] N. Ekici, Z. Kantarci, S. Akyuz. *J. Inclusion Phenom. Mol. Recognit. Chem.*, **10**, 9 (1991).
[44] M. Bakiler, I.V. Maslov, S. Akyuz. *J. Mol. Struct.*, **476**, 21 (1999).
[45] H. Kohler, A. Kolbe, G. Lux. *Z. Anorg. Allg. Chem.*, **428**, 103 (1977).